Kinetic Monte Carlo simulations of the partial oxidation of methanol on oxygen-covered Cu(110)

Christian Sendner,[1] Sung Sakong,[2] and Axel Groß[2]

[1]*Physik-Department T30, Technische Universität München, D-85747 Garching, Germany*
[2]*Abteilung Theoretische Chemie, Universität Ulm, D-89069 Ulm, Germany*

The partial oxidation of methanol to formaldehyde on oxygen-precovered Cu(110) has been studied using kinetic Monte Carlo simulations. The rates entering the simulation have been derived from density functional theory calculations within the generalized gradient approximation using transition state theory. We demonstrate that kinetic Monte Carlo simulations are a powerful tool to elucidate the microscopic details of the reaction kinetics on surfaces. Furthermore, the comparison of calculated and measured temperature programmed desorption rates allows a genuine assessment of the calculated barrier heights.

I. INTRODUCTION

The interaction of methanol with low-index copper surfaces has been a model system for the study of alcohol adsorption on metal surfaces [1–13]. These studies were also motivated by the important role of copper in the synthesis and steam reforming of methanol. Methanol is of particular interest as a means of hydrogen storage in the context of fuel cell technology. Industrially, methanol synthesis and decomposition are promoted by Al_2O_3-supported Cu/ZnO catalysts [14]. However, the precise state of the copper and the role of the ZnO in the Cu/ZnO-catalysts is still unclear. The active phase has been suggested to be either copper dissolved in the bulk [15] or metallic copper dispersed on the ZnO surface [16].

Our knowledge about the oxidation steps of methanol on Cu surfaces is mainly based on temperature programmed desorption (TPD) and scanning tunneling microscopy (STM) experiments. Clean copper surfaces are relatively inactive for methanol oxidation [1–3, 13] while the presence of oxygen strongly promotes the decomposition of methanol on copper [1, 3]. The rate-limiting step in the partial oxidation of oxygen is the methoxy decomposition which was confirmed in electronic structure calculations modeling the Cu surface either by a finite cluster [17–20] or by a periodic slab [21].

We have recently addressed the partial oxidation of methanol on clean and oxygen-covered Cu(100) and Cu(110) in detail using periodic density functional theory (DFT) calculations [22]. The main result of this study was that the promotion of the methanol oxidation on oxygen-covered copper surfaces is not caused by any significant reduction of the methoxy decomposition barrier; instead, oxygen enhances the formaldehyde formation by stabilizing the methoxy intermediate and removing the hydrogen via water desorption.

The reaction pathways determined by the DFT calculations [22] are qualitatively in agreement with the experimental findings. However, the static information obtained from the energetics along the reaction path is not sufficient for a quantitative comparison with experiments. Only a realistic simulation of the experimental situation allows such a comparison. Therefore, we have performed kinetic Monte Carlo simulations of the temperature programmed desorption of methanol from oxygen-covered Cu(110). A very preliminary account of this study will appear somewhere else [23].

Kinetic Monte Carlo (kMC) simulations are a well-accepted theoretical method, for example for the study of growth processes in thin film epitaxy [24–26]. As far as the simulation of chemical reaction kinetics on surfaces is concerned, they have not found a wide-spread recognition yet. In this paper, using the methanol oxidation on oxygen-covered Cu(110) as an example, we will demonstrate that kMC simulations can yield a detailed microscopic insight into rather complex reaction scenarios with competing reaction pathways. Furthermore, they allow a genuine assessment of calculated barrier heights which will be demonstrated by comparing the calculated and measured temperature programmed desorption rates.

This paper is structured as follows. We will first give a brief introduction into the computational details of the kinetic Monte Carlo simulations. We will then discuss the results of the simulations with respect to the partial oxidation and the temperature programmed desorption of methanol on oxygen-covered Cu(110) without and with the presence of a constant hydrogen flux. The paper will end with some conclusions.

II. COMPUTATIONAL DETAILS

Kinetic Monte Carlo simulations can be regarded as a coarse-grained, lattice-based atomistic simulation technique [27]. The first step in any kMC simulation is to set up a list of all possible processes. Every process of the system is described by a rate which can be derived by, e.g., *transition state theory* [28],

$$k_i = k_0 \exp\left(-\frac{E_a}{k_B T}\right) . \tag{1}$$

The rate K_i the probability for the single event i per unit time. E_a is the static energy barrier which has to be crossed, and k_0 is the constant prefactor.

After the event table is set up, one process is chosen with a probability according to its rate. This is done by drawing a random number ρ and selecting the process j that fulfills

$$\sum_{i=1}^{j-1} k_i \leq \rho K < \sum_{i=j}^{N} k_i \qquad (0 \leq \rho < 1) \tag{2}$$

K denotes the overall rate ($K = \sum_{i=1}^{N} k_i$), while N is the number of all possible processes in this system. After this step, the time has to be propagated ($t \rightarrow t + \Delta t$). Assuming that all of these processes are statistically independent from each other, the value of the time step Δt follows Poisson statistics. Therefore it can be chosen by a second random number ρ_2 ($0 \leq \rho_2 < 1$) according to

$$\Delta t = -\ln(1 - \rho_2)/K \ . \tag{3}$$

Finally a new configuration of the systems results and a new event table is to be determined, and then the whole procedure starts again.

For the $CH_3OH/(2 \times 2)O/Cu(110)$ system, a rectangular grid with 60×60 sites in $\hat{x}$- and $\hat{y}$-direction with periodic boundary conditions was chosen. The rates have been derived from periodic DFT calculations [29] using the Perdew-Wang (PW91) functional [30] to treat the exchange-correlation effects within the generalized gradient approximation (GGA). It is well-known that the oxygen-covered Cu(110) surface exhibits a (2×1) "added row" reconstruction consisting of Cu-O-Cu chains [31, 32] which are in a striped phase [33, 34]. Exposure of methanol to oxygen-covered Cu(110) leads to the formation of methoxy-covered regions that are seperated from the oxygen-covered 2×1 striped structures [11]. The formation of the methoxy-covered regions is accompanied by a shrinking of the (2×1)O islands along the stripes in [001] direction [4], i.e. the ends of the (2×1)O correspond to the active area with respect to methoxy formation. These active oxygen areas have been modeled in the DFT calculations by an open $p(2 \times 2)$ oxygen-covered structure (see insets of Fig. 1). For further details of the DFT calculations, we refer to Ref. [22]. To describe the partial oxidation of methanol, we considered the following reactions:

$$\mathrm{CH_3OH^{(a)}} \rightarrow \mathrm{CH_3OH^{(g)}} \tag{4}$$
$$\mathrm{CH_3OH^{(a)}} \rightarrow \mathrm{CH_3O^{(a)} + H^{(a)}} \tag{5}$$
$$\mathrm{CH_3O^{(a)} + H^{(a)}} \rightarrow \mathrm{CH_3OH^{(a)}} \tag{6}$$
$$\mathrm{CH_3O^{(a)}} \rightarrow \mathrm{CH_2O^{(g)} + H^{(a)}} \tag{7}$$
$$\mathrm{CH_3OH^{(a)} + OH^{(a)}} \rightarrow \mathrm{CH_3O^{(a)} + H_2O^{(a)}} \tag{8}$$
$$\mathrm{H_2O^{(a)}} \rightarrow \mathrm{H_2O^{(g)}} \tag{9}$$
$$\mathrm{H^{(a)} + H^{(a)}} \rightarrow \mathrm{H_2^{(g)}} \tag{10}$$
$$\mathrm{CH_3OH^{(g)} + O^{(a)}} \rightarrow \mathrm{CH_3O^{(a)} + OH^{(a)}} \tag{11}$$

In order to locate the transition state configurations and calculate the barrier heights, the climbing image nudged elastic band (NEB) method [35] and the dimer method [36] have been employed. The calculated energetics along the reaction paths on clean and oxygen covered Cu(110) are illustrated in Fig. 1. The barrier heights enter the rates according to Eq. 1. Their values are listed in Table. I. For the prefactor, a generic value of $\nu_0 = 10^{12} s^{-1}$ was assumed for all reactions.

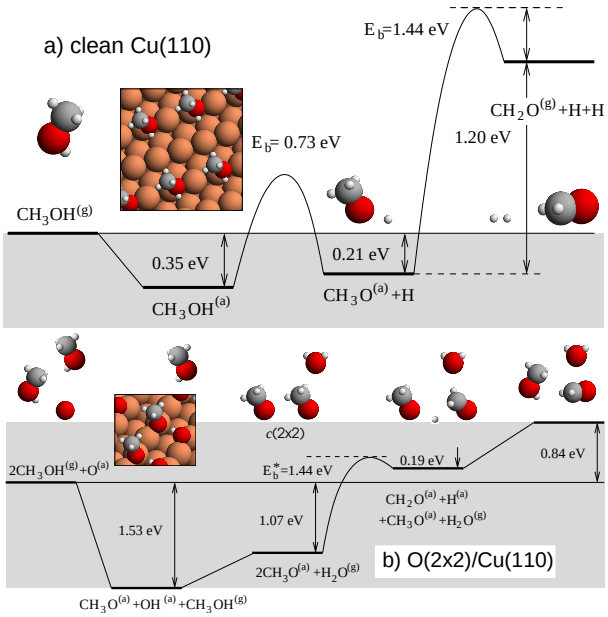

FIG. 1: Reaction pathways of the methanol decomposition on clean (a) and oxygen-covered (b) Cu(110). The (2×2) surface geometry employed in the calculations is illustrated in the insets for the adsorbed methanol molecules on the clean surface in (a) and the dissociated methanol in (b).

In detail, the reactions were modeled in the kMC simulations in the following way. From the gas phase, methanol molecules are adsorbing on the Cu surface with a certain rate. Reaction (4) corresponds to the time-reverse process, the desorption of methanol from clean Cu(110). For reaction (5), the dissociation of methanol into methoxy and hydrogen on clean Cu(110), the methoxy stays at the place of the methanol molecule, while the hydrogen atom occupies one of the four nearest neighbor sites. Only species that are next neighbors are capable to react with each other. If a hydrogen atom is located next to a methoxy molecule, they can build

Reaction	Energy (eV)
(4)	0.35
(5)	0.73
(6)	0.59
(7)	1.44
(8)	0.41
(9)	0.05
(10)	0.75

TABLE I: Energy barriers of the different reactions for methanol on Cu(110), computed by DFT [22].

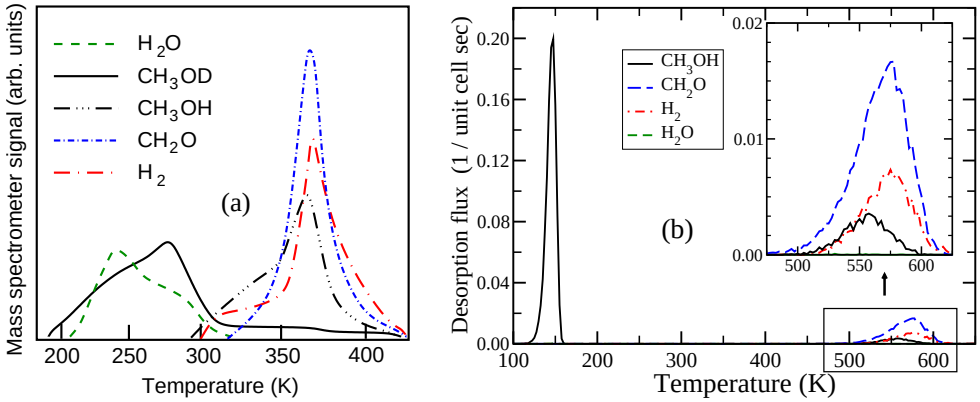

FIG. 2: Temperature programmed desorption spectrum of methanol adsorbed on oxygen-covered Cu(110). a) Experiment (after [1]), b) kinetic Monte Carlo simulation for methanol on (2×2)-oxygen covered Cu(110) based on the DFT barriers listed in table I.

methanol (reaction (6)). The methoxy decomposition (7) into hydrogen and formaldehyde is the rate-limiting step. A diffusing methanol molecule encountering an adsorbed hydroxyl can react to methoxy and water (reaction (8)). Reaction (9) is the water desorption from a $c(2 \times 2)$ methoxy-covered Cu(110) surface, therefore its barrier is rather low. Two hydrogen atoms that meet on the surface can associatively desorb from the surface (reaction (10)). If methanol is impinging on a site which is occupied by oxygen, it reacts spontaneously, i.e. with probability one, to methoxy and OH while the hydroxyl occupies the oxygen site and the methoxy is set on one of the four nearest neighbor sites (reaction (11). This reaction occurs spontaneously (see Fig. 2b).

Besides reacting, the adsorbed species can also diffuse. Since methanol is only weakly bound to the surface, it is able to diffuse with a diffusion barrier of 0.25 eV. Also the hydrogen atoms can diffuse on the surface. The energy barrier used for this process is assumed to be 0.08 eV [37]. This value was computed for H on Cu(100). Probably the diffusion barrier is slightly higher on the more corrugated Cu(110) surface, however, since this barrier is by far the lowest barrier in the simulations, hydrogen diffusion will always be the most probable process so that the hydrogen distribution will correspond to an equilibrium distribution irrespective of the exact barrier height (see discusson below). Furthermore, the DFT calculations yielded a repulsive interaction between methoxy and hydrogen which lies in the range of 0.3 eV [22]. In order to account for this repulsion, the barrier for a hydrogen atom to diffuse to a site adjacent to a methoxy molecule was raised to 0.30 eV.

The diffusion of the hydrogen atoms exhibits by far the lowest energy barrier. This means, that the diffusion rate is very high at temperatures where hydrogen is present on the surface. The rate of the process with the next higher barrier is smaller by a factor which can be up to 10^6 depending on the temperature. Therefore, one has to perform of the order of 10^6 KMC steps until another process than the diffusion occurs. This is computationally very unfavorable. Therefore the diffusion rate was set to zero after 60^2 sequential hydrogen-diffusion events, so that a different process can occur. This corresponds to assuming that hydrogen has reached an equilibrium configuration. By using a higher number of hydrogen diffusion steps, it was checked that this procedure did not influence the configuration of the species on the surface. For each of the spectra presented in the following we averaged over several iterations in order to obtain better statistics.

III. RESULTS

A. Methanol oxidation on the oxygen covered Cu(110) surface

The oxidation of methanol on oxygen-covered Cu(110) was studied experimentally by Wachs and Madix more than 25 years ago [1] by temperature programmed desorption. The results are shown in Fig. 2a. In the experiment, deuterated methanol was used in order to identify the nature of the dissociation processes. Theoretically, we have obtained the TPD spectrum by performing KMC simulations using the DFT energies in table I for a Cu(110) surface precovered with 0.25 ML oxygen in a (2×2) structure. A methanol flux of 0.1 ML/s for 100 s at 100 K was applied to cover the surface with methanol. Then, the surface was heated with a rate of 5 K/s.

The results of this simulation are shown in Fig. 2b. The comparison between theory and experiment reveals large quantitative and also qualitative differences. In the simulations, upon the exposure at 100 K methanol molecules that impinge at oxygen atoms adsorb dissociatively as methoxy and OH. The methoxy concentration on the surface becomes 20%. Methanol also adsorbs molecularly, i.e. intact, on the oxygen-free sites with a concentration of 55%. At 120 K, methanol starts to desorb in the simu-

lations with the peak at 145 K whereas in the experiment it only desorbs considerably above 200 K.

Furthermore, while in the experiment water desorbs in the same temperature range as methanol, there is no water desorption in the simulations. Since the barrier for the water formation from methanol and OH (reaction (5)) is 0.06 eV higher than the barrier for methanol desorption, almost no water is formed. Therefore it cannot desorb, even with the low barrier for water desorption from the methoxy $c(2\times2)$ structure. At 160 K, the whole methanol is desorbed from the surface. Only if the energy barrier for the reaction of methanol and hydroxyl to water and methoxy is lower than the desorption barrier for methanol, water is produced by reaction (8). We tested this by lowering the barrier for reaction (8) from 0.41 eV to 0.30 eV. Then H_2O is produced at 130 K and desorbs directly from the surface. In addition, more methoxy is built by reaction (8) raising the concentration of methoxy from 20 % at 100 K to 40 % at 150 K.

For temperatures above 500 K methoxy starts to decompose into formaldehyde and hydrogen in the calculations (reaction (7)). Formaldehyde becomes the main desorption product, but since hydrogen becomes available again, these atoms can react with the adsorbed methoxy to methanol or, if two hydrogen atoms are next neighbors, they can associatively desorb. However, in the experiment the formaldehyde formation already starts at 350 K which indicates that the calculated energy barrier of 1.44 eV for the methoxy decomposition is certainly too high. Still the relative heights of the desorption peaks of methanol, formaldehyde and hydrogen are well-reproduced by the calculations.

In fact, it is really surprising that a H_2-peak is visible in the simulated TPD-spectra (Fig. 2b). Note that the energy barrier for the recombinative hydrogen desorption is 0.75 eV which is 0.16 eV higher than the barrier for methanol formation from hydrogen and methoxy. This means that the rate for H_2 desorption is significantly lower than for methanol desorption. Furthermore, the concentration of methoxy on the surface is much higher than the concentration of the hydrogen atoms which is always less than 2.5 %. The reason for the significant fraction of desorbing hydrogen molecules is the repulsive interaction between methoxy and hydrogen [22] which makes a configuration with a hydrogen atom and a methoxy radical very improbable. This suppresses the associative desorption of methanol so that the flux of H_2 and methanol desorption become comparable. Without this repulsive interaction, the H_2 desorption flux is much smaller, as we checked by performing corresponding kinetic Monte Carlo simulations.

As already mentioned, the comparison between theory and experiment (Fig. 2) is certainly not satisfactorily. However, as should have become obvious from the discussion so far, the TPD spectrum of methanol adsorbed on oxygen-covered Cu(100) is the result of a complex reaction scenario with many interconnected processes. In order to identify the reasons for the discrepancies between theory and experiment, we have tried to readjust the calculated barrier heights in order to get a better agreement. As it turns out, the most crucial discrepancies are due to the underestimation of the methanol adsorption energy and the overestimation of the barrier for methoxy decomposition. In addition, some fine tuning had to be made in order to reproduce further details of the experimental TPD spectrum.

We will now discuss in detail the adjustments that have been made in order to improve the agreement between experiment and theory. According to experiments [6, 38], water desorbs at temperatures of 160 - 170 K from a clean Cu(110) which corresponds to an energy barrier of about 0.4 eV. For the partial oxidation of methanol on the oxygen-covered Cu surface, this peak only appears at temperatures higher than 200 K (Fig. 2a). This is an indication that water is created by reaction (8) at that temperature and then desorbs. In order to reproduce the water and the first methanol desorption peaks, the energy barrier for the water production (8) has been increased to 0.58 eV and the barrier for methanol desorption to 0.65 eV. For the barrier for water desorption (9) the value for the clean surface has now been taken although the exact value of this barrier hardly influences the results as long as it is below the barrier for the water production. The activation energies for the diffusion and the associative desorption of hydrogen have been left unchanged.

Because of the increased adsorption energy of methanol, the barrier for the dehydrogenation of methanol is also increased by 0.22 eV (reaction 5), and the same is true for the corresponding back reaction, the recombination of hydrogen and methoxy (6). As a further consequence, the methanol diffusion barrier was set to 0.50 eV. As far as the barrier for the methoxy decomposition is concerned (reaction (7)), we lowered it significantly to 0.90 eV.

The adjusted barrier heights are listed in Table II, and the resulting calculated TPD spectrum is shown in Fig. 3a. Now the main features of the experimental spectrum are reproduced on a semi-quantitative level. Water desorbs at 245 K, and the first methanol desorption peak appears at 270 K. The reduced methoxy decomposition barrier leads to lower desorption temperatures of formaldehyde, methanol and hydrogen with peaks between 350 and 370 K, in accord with the experiment.

Reaction	**Energy (eV)**
(4)	0.65
(5)	0.95
(6)	0.81
(7)	0.90
(8)	0.58
(9)	0.40
(10)	0.75

TABLE II: Suitable energy barriers to reproduce the experimental results.

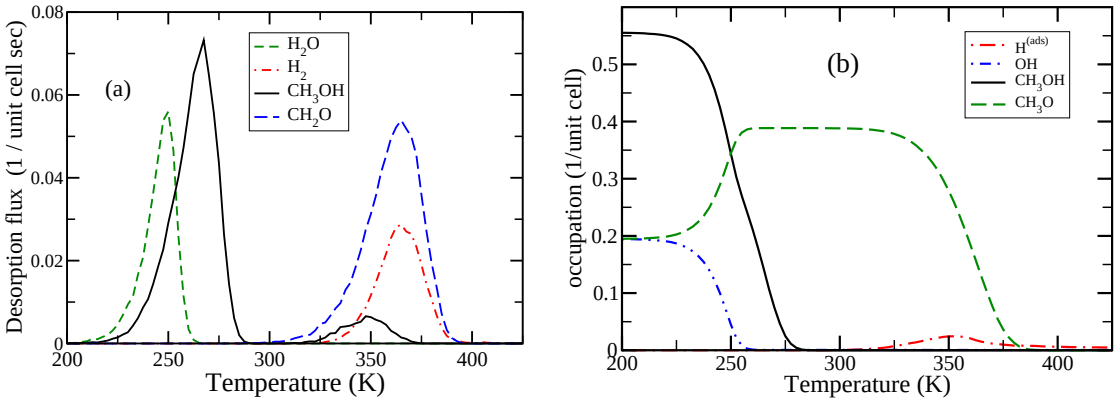

FIG. 3: Temperature programmed desorption of methanol adsorbed on oxygen-covered Cu(110) using the energy barriers of table II. a) Simulated TPD-spectrum. A flux of 0.1 ML/s methanol was applied for 100 s at 180 K to the surface, which was covered with 0.25 ML oxygen. Afterwards, the heating rate was 5 K/s. b) Concentration of various species during the TPD simulation.

The H_2 desorption flux is larger and at a slightly higher temperature than the methanol desorption, also in agreement with the experiment,

In addition to the simulated TPD spectrum, in Fig. 3b the concentration of the different species on the surface during the TPD run is shown. After deposition of the methanol, again a methanol concentration of 55 % and a methoxy concentration of 20 % result. When the methanol starts to desorb at 220K, the methanol concentration begins to decrease. The methanol concentration also starts to decrease because of the formation of methoxy and water according to reaction (8). This leads to an increase in the methoxy concentration. The concentration of the formed water molecules does not show up because the water molecules immediately desorb after their formation.

At about 320 K, the methoxy decomposition into hydrogen and formaldehyde starts; therefore the methoxy concentration begins to decrease. There is no significant concentration of formaldehyde on the surface because it immediately desorbs after its formation. The hydrogen atoms, on the other hand, have to find either another hydrogen atom or a methoxy radical before they desorb recombinatively as molecular hydrogen or methanol, respectively. Since the hydrogen atoms do not immediately find a reaction partner, a small concentration of diffusing hydrogen atoms builds up.

There are still quantitative differences between theory and experiment. In particular, the widths of the water and the first methanol desorption peaks are too small; furthermore, their heights are too large compared to the formaldehyde desorption peak. This is simply due to the fact that we did not take into account any lateral interaction between the adsorbed water and methanol molecules which would lead to a broadening and lowering of the desorption peaks [39]. In fact, TPD spectra of methanol desorbing from Cu(110) show a dependence of their shape on the coverage [40] indicating the role of the mutual interaction between the adsorbed methanol molecules.

B. Desorption of methanol under a constant hydrogen flux

When the oxygen-covered Cu(110) surface is exposed to methanol at 180 K, the adsorbed species are methanol, methoxy and hydroxyl. According to the reaction pathways in Fig. 1, upon heating of the system the adsorbed methoxy radical should recombine with hydrogen and desorb as methanol rather than decompose to formaldehyde since the barrier for the methoxy decomposition is higher than for the methanol recombination and desorption. However, the pathway for methanol recombination is not available since all adsorbed hydrogen atoms desorb as water. Only if additional hydrogen is offered, the methanol recombination can occur before the methoxy decomposition.

This pathway was in fact already tested in the experiments by Wachs and Madix [1] in which after the adsorption of 2 Langmuir oxygen and 100 seconds of methanol flux at 180 K a pressure of 10^{-6} Torr of deuterium was applied. The measured TPD spectrum of methanol showed two broad peaks. The first one was centered at 270 K like the first methanol peak in Fig. 2a which means that it corresponds to the desorption of molecularly adsorbed methanol. The second peak was centered around 360 K and attributed to the desorption of methanol originating from the recombination of methoxy and hydrogen.

We also addressed this experimental setup in our simulations. After the dosage of methanol on the oxygen covered surface, a constant flux of hydrogen atoms of 0.04 ML/s was applied while heating the surface which corresponds roughly to the experimental pressure. The hydrogen flux leads to a considerable concentration of up to a quarter monolayer of hydrogen atoms on the surface so that the recombination of methoxy and hydrogen (reaction (6)) becomes possible.

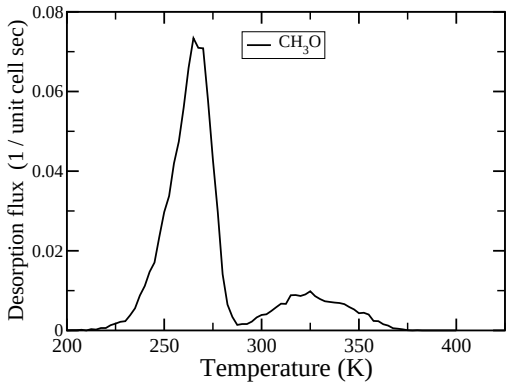

FIG. 4: Calculated temperature programmed desorption spectrum of methanol under a constant hydrogen flux with the energy barriers of table II. After the methanol adsorption during 100 s on the oxygen covered surface, the surface was heated with 5 K/s while a flux of 0.04 ML/s hydrogen was applied.

Using the DFT barriers of table I, two well-separated methanol desorption peaks appear, the first one being almost the same as in Fig. 2a, and the second one is peaked at about at 240 K, caused by the recombination of methoxy and hydrogen to methanol. Thus our simulations confirmed the assignment of the experimental peaks [1], however, the desorption temperatures of the simulations are too low. With the adjusted barriers listed in table II, the agreement between experiment and simulations becomes much better. The resulting calculated TPD spectrum of methanol is shown in Fig. 4.

The general features of the experiment are reproduced. Still there are again quantitative differences. As far as the second peak is concerned, its position is too low by about 30 K and its intensity is too small. Furthermore, in the experiment the second peak extends up to temperatures of more than 420 K. In our simulations, at these high temperatures the methoxy concentration on the surface is dramatically reduced due to the decomposition reaction (7). In addition, hydrogen also disappears from the surface because of associative desorption. With almost no methoxy and hydrogen present on the surface, the recombinative desorption according to reaction (6) can not occur any more.

IV. DISCUSSION AND CONCLUSIONS

Our kinetic Monte Carlo simulations of the temperature programmed desorption of methanol dosed on oxygen-covered Cu(110) have shown that using the activation barriers from DFT calculations leads to quantitative and qualitative discrepancies with the experiment. Still certain features of the experimental TPD spectrum are well-reproduced, for example the branching ratio between methanol, formaldehyde and hydrogen desorption at high temperatures after the methoxy decomposition. The simulations indicate that the relative small flux of recombinative methanol desorption at high temperatures is due to the repulsion between hydrogen and methoxy on the surface which was derived from the DFT calculations.

In order to analyse the error on the used barrier heights quantitatively, we have adjusted the barriers so that better agreement with the experiment was achieved. We performed two main adjustments. First the methanol adsorption energy was increased by 0.3 eV so that the molecular methanol desorption occurs at higher temperatures. Secondly, the barrier for methoxy decomposition was singnificantly reduced by more than 0.5 eV. With these adjustments and further fine tuning, the experiments could be satisfactorily reproduced.

There are two possible main reasons for the severe adjustments: either the reaction bariers calculated by DFT are inaccurate, and/or the reactions in the experiment were dominated by active defect sites that were not included in the simulations. We first discuss possible errors in the DFT barrier heights. As far as the barrier for C-H bond scission is concerned, it is a well-known fact that DFT calculations using the GGA for the exchange-correlation effects overestimate the barrier for C-H bond scission in many systems, for example, for the C-H bond breaking of ethylene (C_2H_4) to vinyl (C_2H_3) on Pd(111) [41] and for the methane (CH_4) decomposition on Ni(111) [42]. Hence the used DFT exchange-correlation functional [30] might indeed not be appropriate for the description of the C-H bond scission.

However, it might also well be that some crucial processes in the partial oxidation of methanol on oxygen-covered Cu(110) were not considered in our kMC study. The quality of kMC simulations is essentially dependent on the list of processes considered. We had modeled the active oxygen species at the end of the (2×1)O stripes [4] by an open $p(2 \times 2)$ oxygen structure, but this might be an inappropriate model. Furthermore, the reactions in the experiment might be dominated by active defect sites that were not included in the simulations. For example, it is well-known that adsorption energies can be considerably higher at step sites than at flat terraces [43–45]. In addition, dissociation barriers can be significantly lower at steps so that they dominate the dissociation kinetics [46, 47]. We are planning to address these issues in the partial oxidation of methanol on oxygen-covered Cu(110) by determining the reaction pathways on a realistic (2×1)O phase on Cu(110) and on stepped Cu surfaces.

Apart from DFT errors and additional reaction sites also the inclusion of lateral interaction between the adsorbates can considerably influence the simulated desorption spectra by changing both the width as well the position of the TPD peaks. Except for the interaction between adsorbed hydrogen and methoxy we have not calculated any lateral interactions which explains the reduced widths of our calculated desorption peaks compared to the experiment. Furthermore, lateral interactions could also be the

source of the discrepancy between theory and experiment in the position of the low-temperature methanol desorption peak. In fact, on clean Cu(110) the methanol desorption is peaked around 180 K [40] from which a methanol adsorption energy of 0.45 eV was derived, in good agreement with the DFT value of 0.35 eV [22]. Obviously, the oxygen coverage of the Cu surface does not only lead to the spontaneous dissociation of methanol impinging close to the adsorbed oxygen atoms (see Fig. 1) but also to a stabilization of molecularly adsorbed methanol.

In spite of these uncertainties, we are convinced that the kinetic Monte Carlo simulations have given valuable insights into the complex details of the reaction dynamics and kinetics of the partial oxidation of methanol on oxygen-covered Cu(110) which can not be obtained from the static information of total energy calculations alone.

Acknowledgments

This work has been supported by the German Academic Exchange Service (DAAD) and the German Science Foundation (DFG, GR1503/12-2).

[1] Wachs, I. E.; Madix, R. J. *J. Catal.* **1978**, *53*, 208.
[2] Bowker, M.; Madix, R. J. *Surf. Sci.* **1980**, *95*, 190.
[3] Sexton, B. A.; Hughes, A. E.; Avery, N. R. *Surf. Sci.* **1985**, *155*, 366.
[4] Leibsle, F. M.; Francis, S. M.; Davis, R.; Xiang, N.; Haq, S.; Bowker, M. *Phys. Rev. Lett.* **1994**, *72*, 2569.
[5] Madix, R. J.; Telford, S. G. *Surf. Sci.* **1995**, *328*, L576.
[6] Carley, A. F.; Davies, P. R.; Mariotti, G. G.; Read, S. *Surf. Sci.* **1996**, *364*, L525.
[7] Poulston, S.; Jones, A. H.; Bennett, R. A.; Bowker, M. *J. Phys.: Condens. Matter* **1996**, *8*, L765.
[8] Davies, P. R.; Mariotti, G. G. *Catal. Lett.* **1997**, *43*, 261.
[9] Bowker, M.; Poulston, S.; Bennett, R. A.; Jones, A. H. *Catal. Lett.* **1997**, *43*, 267.
[10] Silva, S. L.; Lemor, R. M.; Leibsle, F. M. *Surf. Sci.* **1999**, *421*, 135.
[11] Silva, S. L.; Lemor, R. M.; Leibsle, F. M. *Surf. Sci.* **1999**, *421*, 146.
[12] Karolewski, M. A.; Cavell, R. G. *Appl. Surf. Sci.* **2001**, *173*, 151.
[13] Ammon, C.; Bayer, A.; Held, G.; Richer, B.; Schmidt, T.; Steinrück, H. P. *Surf. Sci.* **2002**, *507*, 845.
[14] Vanden Bussche, K. M.; Froment, G. G. *J. Catal.* **1996**, *161*, 1.
[15] Klier, K. *Adv. Catal.* **1982**, *31*, 243.
[16] Chinchen, G. C.; Hay, C. M.; Vandervell, H. D.; Waugh, K. C. *J. Catal.* **1987**, *103*, 79.
[17] Witko, M.; Hermann, K. *J. Chem. Phys.* **1994**, *101*, 10173.
[18] Gomes, J. R. B.; Gomes, J. A. N. F.; Illas, F. *Surf. Sci.* **1999**, *443*, 165.
[19] Gomes, J. R. B.; Gomes, J. A. N. F. *Surf. Sci.* **2001**, *471*, 59.
[20] Nakatsuji, K.; Hu, Z.-M. *Int. J. Quantum. Chem.* **2000**, *77*, 341.
[21] Greeley, J.; Nørskov, J. K.; Mavrikakis, M. *Annu. Rev. Phys. Chem.* **2002**, *53*, 319.
[22] Sakong, S.; Groß, A. *J. Catal.* **2005**, *231*, 420.
[23] Sakong, S.; Sendner, C.; Groß, A. J. Mol. Struct. (THEOCHEM), accepted for publication.
[24] Fichthorn, K. A.; Scheffler, M. *Phys. Rev. Lett.* **2000**, *84*, 5371.
[25] Bogicevic, A.; Ovesson, S.; Hyldgaard, P.; Lundqvist, B. I.; Brune, H.; Jennison, D. R. *Phys. Rev. Lett.* **2000**, *85*, 1910.
[26] Piana, S.; Gale, J. D. *J. Am. Chem. Sc.* **2005**, *127*, 1975.
[27] Fichthorn, K. A.; Weniberg, W. H. *J. Chem. Phys.* **1991**, *95*, 1090.
[28] Hänngi, P.; Talkner, P.; Borkovec, M. *Rev. Mod. Phys.* **1990**, *62*, 251.
[29] Kresse, G.; Furthmüller, J. *Phys. Rev. B* **1996**, *54*, 11169.
[30] Perdew, J. P.; Chevary, J. A.; Vosko, S. H.; Jackson, K. A.; Pederson, M. R.; Singh, D. J.; Fiolhais, C. *Phys. Rev. B* **1992**, *46*, 6671.
[31] Coulman, D. J.; Wintterlin, J.; Behm, R. J.; Ertl, G. *Phys. Rev. Lett.* **1990**, *64*, 1761.
[32] Jensen, F.; Besenbacher, F.; Lægsgaard, E.; Stensgaard, I. *Phys. Rev. B* **1990**, *41*, 10233.
[33] Kern, K.; Niehus, H.; Schatz, A.; Zeppenfeld, P.; Goerge, J.; Comsa, G. *Phys. Rev. Lett.* **1991**, *67*, 855.
[34] Bombis, C.; Moiseeva, M.; Ibach, H. *Phys. Rev. B* **2005**, *72*, 245408.
[35] Henkelman, G.; Uberuaga, B. P.; Jónsson, H. *J. Chem. Phys.* **2000**, *113*, 9901.
[36] Henkelman, G.; Jónsson, H. *J. Chem. Phys.* **1999**, *111*, 7010.
[37] Sakong, S.; Groß, A. *Surf. Sci.* **2003**, *525*, 107.
[38] Lackey, D.; Schott, J.; Straehler, B.; Sass, J. *J. Chem. Phys.* **1989**, *91*, 1365.
[39] Stampfl, C.; Kreuzer, H. J.; Payne, S. H.; Pfnür, H.; Scheffler, M. *Phys. Rev. Lett.* **1999**, *83*, 2993.
[40] Peremans, A.; Dereux, A.; Maseri, F.; Darville, J.; Gilles, J.-M.; Vigneron, J.-P. *Phys. Rev. B* **1992**, *45*, 8598.
[41] Pallassana, V.; Neurock, M.; Lusvardi, V. S.; Lerour, J. J.; Kragten, D. D.; van Santen, R. A. *J. Phys. Chem. B* **2002**, *106*, 1656.
[42] Kratzer, P.; Hammer, B.; Norskøv, J. K. *J. Chem. Phys.* **1996**, *105*, 5595.
[43] Gambardella, P.; Šljivančanin, Ž.; Hammer, B.; Blanc, M.; Kuhnke, K.; Kern, K. *Phys. Rev. Lett.* **2001**, *87*, 056103.
[44] Schmidt, P. K.; Christmann, K.; Kresse, G.; Hafner, J.; Lischka, M.; Groß, A. *Phys. Rev. Lett.* **2001**, *87*, 096103.
[45] Lischka, M.; Groß, A. *Phys. Rev. B* **2002**, *65*, 075420.
[46] Dahl, S.; Logadottir, A.; Egeberg, R. C.; Larsen, J. H.; Chorkendorff, I.; Törnqvist, E.; Nørskov, J. K. *Phys. Rev. Lett.* **1999**, *83*, 1814.
[47] Groß, A. *Surf. Sci.* **2002**, *500*, 347.